Piezoresistive and Piezoelectric MEMS Strain Sensors for Vibration Detection

Stanley Kon[a], Kenn Oldham[b] and Roberto Horowitz[a]

[a]Computer Mechanics Laboratory, University of California, Berkeley, CA 94720;
[b]Army Research Lab, 2800 Powder Mill Road, Adelphi, MD 20783

ABSTRACT

Both piezoresistive and piezoelectric materials are commonly used to detect strain caused by structural vibrations in macro-scale structures. With the increasing complexity and miniaturization of modern mechanical systems such as hard disk drive suspensions, it is imperative to explore the performance of these strain sensors when their dimensions must shrink along with those of the host structures. The miniaturized strain sensors must remain as small as possible so as to minimum their effect on structure dynamics, yet still have acceptable sensing resolution. The performances of two types of novel micro-scale strain gage for installation on stainless steel parts are compared in this paper. Micro-fabrication processes have been developed to build polycrystalline silicon piezoresistive strain sensors on a silicon substrate, which are later bonded to a steel substrate for testing. Piezoresistor geometries are optimized to effectively increase the gage factor of piezoresistive sensors while reducing sensor size. The advantage and disadvantage of these piezoresistors are compared to those of piezoelectric sensors. Experimental results reveal that the MEMS piezoelectric sensors are able to achieve a better resolution than piezoresistors, while piezoresistors can be built in much smaller areas. Both types of the MEMS strain sensors are capable of high sensitivity measurements, subject to differing constraints.

Keywords: piezoelectric sensor, piezoresistor, strain gage, ZnO, piezoresistive, vibration

1. INTRODUCTION

Vibrations are a common phenomena of mechanical structures that can be detrimental to many systems. Hard disk drives, for example, are extremely sensitive to both external vibrations[1] and to airflow-induced vibration of the metal suspensions that carry the drive's read/write heads.[2] The suspension vibrations prevent the accurate positioning of the head, resulting in an erroneous reading/writing signal; the external vibration may even cause heads to crash into the disk, a catastrophic failure for hard disk drives. Hence, vibration monitoring is a key to insuring system robustness and enhancing overall performance for applications of this kind.

Various methodologies have been developed to measure vibrations. Laser vibrometers compare the frequency shift between the outgoing and reflected laser beam and the corresponding vibration velocity is evaluated. These instruments can take very accurate measurement if the measured surface is reasonably reflective and the laser beam is properly aligned. The non-contact nature of this measurement is the major advantage over other types of vibration measurements. However, these instruments are too bulky to fit into small machineries. Another methodology measures strain induced by the mechanical vibrations of the structure. In this case, sensors are applied to the mechanical structure to be monitored. Assuming the presence of sensors has a negligible effect on the structure, the true strain can be measured by monitoring the electrical signals passing through the sensors, and related to vibration of the structure. Piezoresistive and piezoelectric materials are the most common sensor materials used in this kind of measurement.

Conventionally, a completed piezoresistor is sandwiched between two transparent insulation layers. The piezoresistor is attached to the host structure using adhesives prior to measurement. While this works well for relatively large structures such as specimens for tensile strength tests, this method is not appropriate for smaller structures as the sensor size becomes more dominant relative to the structure; as the host structure shrinks, even the adhesives can be too thick to avoid influencing behavior of the underlying substrate. Therefore, the

E-mail: horowitz@me.berkeley.edu, Telephone: 1 510 642 4675

Sensors and Smart Structures Technologies for Civil, Mechanical, and Aerospace Systems 2007,
edited by Masayoshi Tomizuka, Chung-Bang Yun, Victor Giurgiutiu, Proc. of SPIE Vol. 6529,
65292V, (2007) · 0277-786X/07/$18 · doi: 10.1117/12.715814

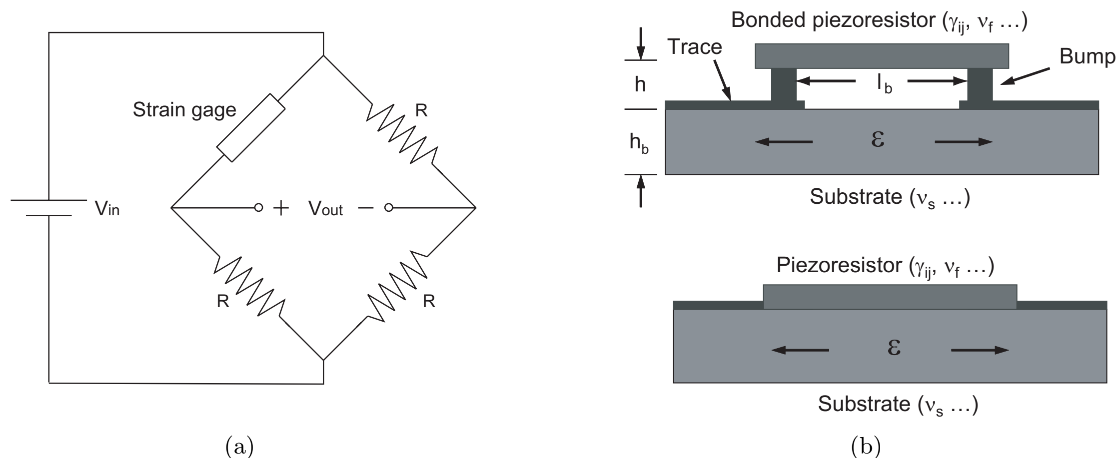

Figure 1. (a) One type of Wheatstone bridges for strain measurement; (b) Schematic drawing of a bonded piezoelectric strain gage (top) and a conventional thin film strain gage (bottom).

overall sensor size must shrink along with the host structure. For structures such as hard disk drive suspensions, which are composed of metal sheets ranging from 40 to 300 μm thick, this means the sensor thickness should be no more than a few microns. In addition, a more important reason is that there are typically optimal sensor locations[3,4,5,6] to place vibration sensors on mechanical structures. The optimal sensor location is a function of structure geometry and the intended vibration signal to be retrieved. It is desirable to choose a sensor location such that only the vibrations of interests are detected by the strain sensors. This optimal sensor location theory, however, requires sensors to be much smaller than the host structure. Hence, the proper way to implement these sensor schemes on small structures is to shrink sensors in all dimensions.

Micro-electro-mechanical systems (MEMS) fabrication techniques can be useful in these situations for their ability to build very small sensors with precise geometries. Furthermore, many sensor technologies have been developed using specialized sensor materials, such as high-quality semiconductors, and piezoelectric thin films. Both silicon piezoresistors and piezoelectric thin films have been used to measure vibrations at the micro-scale, in such applications as accelerometers and resonators.[7] However, to expand their use to general mechanical parts requires adapting standard micro-scale fabrication techniques to new environments and substrates.

In this paper, we explore the use of piezoelectric and piezoresistive strain sensors for vibration detection at micro scale. First, we present the theory and a novel design of piezoresistive MEMS sensors which effectively increases the gage factor, followed by piezoelectricity theory and piezoelectric sensor modeling. In the second section, a method of micro-fabricating and transferring them to steel substrates is detailed. This fabrication strategy ensures a high quality piezoresistive film and precise strain sensor geometries. Fabrication of ZnO sensors directly on steel substrates is also demonstrated in this section. In the third section, we show the experimental setup and results for both sensor types, compare the different characteristics and discuss the resolution constraints on each sensor at MEMS scale. The last section concludes the paper.

2. THEORY

2.1. Piezoresistive Effects in Thin Films

2.1.1. Gauge Factor of Bonded Piezoresistors

The piezoresistive effect describes the change of material electrical resistance owning to external stress or material deformation. As a sensor, this effect is commonly measured utilizing Wheatstone bridge circuits. Several variations of Wheatstone bridge are used under different circumstances. Fig. 1(a) shows one of the configurations in which only a single piezoresistor is implemented on the circuit. When the sensor resistance is changed due to piezoresistive effects, it causes the voltage on the voltage divider to change. The resistance change and the amount of strain are calculated backwards by compare this voltage change to the reference voltage divider. The

sensitivity of a piezoresistive sensor is quantified as gauge factor, which is defined as the percentage change in resistance per unit strain, or in equation:

$$G = \frac{\Delta R/R}{\epsilon} = k_l K_b K_g \tag{1}$$

where k_l, K_b, and K_g are the constants that will be discussed in the following paragraphs. In general, the percentage change in resistance, $\Delta R/R$, can be re-written by taking the derivative of the formula $R = \rho l/A$,

$$\frac{\Delta R}{R} = \frac{\Delta\rho}{\rho} + \frac{\Delta(l/A)}{l/A} = \frac{\Delta\rho}{\rho} + (\frac{\Delta l}{l} - \frac{\Delta A}{A}) \tag{2}$$

where l, A, and ρ are sensor length, cross-sectional area and resistivity, respectively. The change in resistivity may be related as follows,[8]

$$\frac{\Delta\rho_i}{\rho} = \sum_{j=1}^{6} \gamma_{ij}\varepsilon_j \tag{3}$$

where i and j take values from 1 to 6, denoting the parameters in the corresponding strain direction and γ is the electroresistance coefficient. Material such as single crystal silicon has a cubic crystal structure, of which γ can be described using three constants γ_{11}, γ_{12}, and γ_{44}. For a free standing piezoresistor under uniaxial loading, $\frac{\Delta l}{l} = \varepsilon_1 = \varepsilon$, $\varepsilon_2 = \varepsilon_3 = -\nu\varepsilon$ and $\frac{\Delta A}{A} = -2\mu\varepsilon$, Eq. (3) can be written as

$$k_{l,free} = \frac{\Delta R}{R\epsilon_1} = \gamma_{11} - 2\nu_f\gamma_{12} + 3 \tag{4}$$

where ν_f is the thin film Poisson's ratio. This resembles the configuration of bonded strain gages, which consist of a thin film piezoresistive element attached to a substrate at each end through an elevated metal bond, as shown in the top half of Fig. 1(b). The strain gage is bonded to the substrate through metal-to-metal bonding, on top of an insulation layer coating the steel substrate. The metal bonding allows current to pass through the piezoresistor suspended across the bonds. Bonded gage behaves differently from conventional strain gages that are in contact with their substrate continuously. In the latter case, $\nu_h = -\nu_f(1-\nu_s)/(1-\nu_f)$ is a function of both Poisson's ratio of the substrate and the sensor.[9] The longitudinal gage factor of this type under uniaxial loading is given by

$$k_{l,film} = \frac{\Delta R}{R\epsilon_1} = \gamma_{11} - (\nu_f + \nu_h)\gamma_{12} + 1 + \nu_s + \nu_h \tag{5}$$

$$\nu_h = \frac{1-\nu_s}{1-\nu_f}\nu_f \tag{6}$$

where ν_s is the substrate Poisson's ratio. Since Poisson's ratios are smaller than unity, it is notable that, depending on the piezoresistance coefficient, the same sensor under uniaxial load may effectively have a slightly higher gage factor in the bonding configuration than in the traditional contact configuration shown in the bottom half of Fig. 1(b).

The strain on the sensors may also be mechanically amplified by the added sensor height due to the bonds, especially when subjected to bending. The phenomenon becomes more dominant as the bond becomes higher. However, the introduction of the bonds has one drawback for sensor operation. In the bonded sensor configuration, the total deformation of the sensor due to strain is the sum of the deformation of the piezoresistor and of the two bonds. The deformation on the bonds inevitably reduces the amount of displacement transferred to the sensors, resulting a lower strain level. This factor can be estimated as

$$K_b = \frac{1}{1 + \frac{2h}{l_b}\frac{A_s E}{A_b G}} \tag{7}$$

where h, l_b, A_s, A_b, E, and G are bond height, sensor length, sensor cross-sectional area, bond area, piezoresistor Young's modulus and shear modulus of the bonding metal. This factor reduces to unity in the extreme case when the bonding metal is much more stiff than the sensor material, $G >> E$. In other words, it appears the sensor follows the exact substrate displacement. Conversely, the gage sensitivity will be greatly reduced if the bond height is substantially larger than the sensor length, $h >> l_b$, as $K_b \to 0$ in this case.

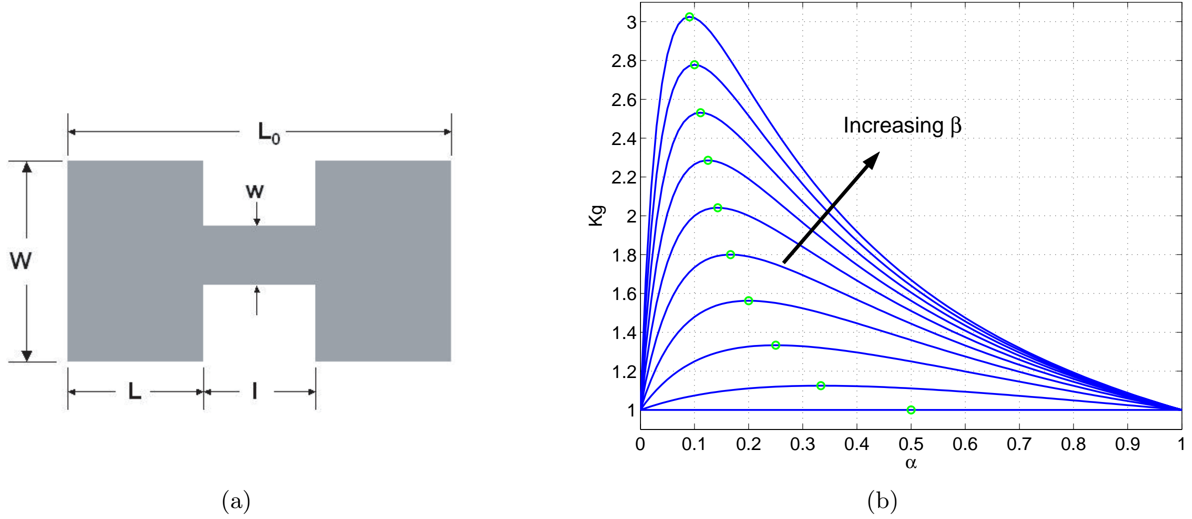

Figure 2. (a) Dogbone geometry for gage factor amplification; (b) The geometry amplification factor K_g versus α.

2.1.2. Gage Factor Amplification Through Sensor Design

Gage factor of piezoresistive strain gages can be effectively increased through innovations in sensor geometry. The modified design features a dog-bone shaped resistor, as shown in Fig. 2(a). The total resistance, $R_g = 2R_w + R_t$, for the dog bone sensor is the sum of the resistance from the two wider sections, $2R_w$, plus the resistance of middle section, R_t. It is assumed that the sensor layer is much thinner than the underlying substrate. When a load is applied at the ends of the sensor, the sensor can be modeled as three springs, which corresponds to the three sections mentioned above, connected in series. Each of the section is subject to the same amount of force. Since the middle section has the smallest cross section, it will elongate more than the other two, resulting a larger strain. The relation between the true strain on the structure, ε, measured from the ends and the strain from each section can be expressed as follows:

$$\varepsilon_t = \frac{L_0}{2\frac{w}{W} + l}\varepsilon \tag{8}$$

$$\varepsilon_w = \frac{w}{W}\varepsilon_t \tag{9}$$

where ε_t, ε_w, and L_0 are the strain at the middle section, the strain at the wider section and the sensor total length. The amount of increase in sensitivity can be evaluated as:

$$K_g = \frac{1 + (\beta^2 - 1)\alpha}{[1 + (\beta - 1)\alpha]^2} \tag{10}$$

$$\text{where} \quad \alpha = \frac{l}{l + 2L} = \frac{l}{L_0}; \quad \beta = \frac{W}{w} \tag{11}$$

Fig. 2(b) shows the relation between K_g and α for various thickness ratios, $\beta \geq 1$. Intuitively, the ideal way to maximize this effect is to make the middle section thinner so that most of the deformation occurs at this section. Fabrication feasibility and thermal noise are the main factors that form the limitation of the middle section dimensions. It is more difficult to pattern a thinner section in lithography and etching steps. A thinner section also generates more heat during measurements as the current needs to pass through a smaller area. The heat causes sensor temperature to raise which impairs measurements due to the increasing thermal noise.

2.2. Piezoelectric Effects in Thin Films

Piezoelectricity arises from the cross-coupling of mechanical and electrical energy within certain materials; these materials can be used as both actuators and sensors. When a piezoelectric device is used as sensors, it actively

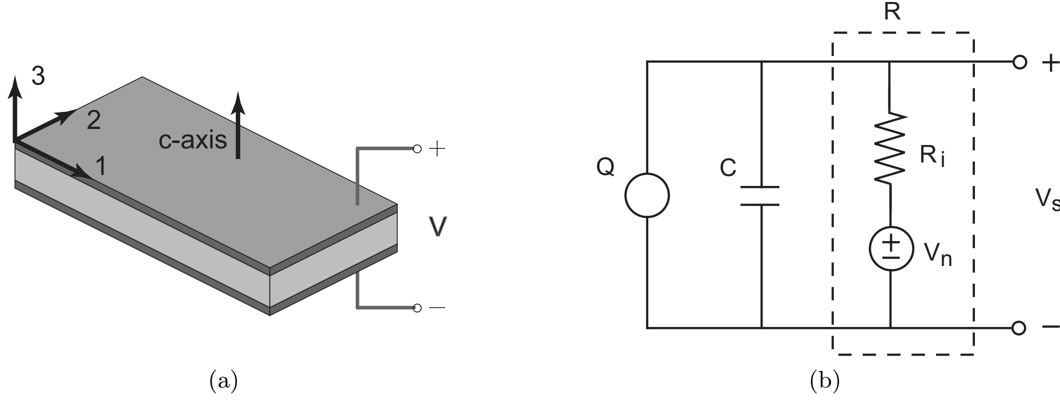

Figure 3. (a) Schematic drawing of a conventional MEMS piezoelectric sensor; (b) The piezoelectric sensor model.

generates charges in response to external loads, as compared to piezoresistive sensors where a voltage source is applied across the sensor to measure the strain. This cross-coupling from mechanical to electrical energy is called the direct piezoelectric effect. The constitutive equation is given as follows[10]:

$$D_i = e_{ij} S_j + \epsilon_0 \epsilon_{ik}^S E_k \tag{12}$$

where D and S are electric displacement and mechanical strain, respectively. The subscripts $i = 1, 2, 3$, $k = 1, 2, , 3$, and $j = 1, 2, 3, 4, 5, 6$ denote the direction to which physical properties are related. The constant, ϵ_0, is the permittivity of the free space whereas ϵ_{ik}^S is the relative permittivity at constant strain. The strain piezoelectric coefficient, e_{ij}, relates the amount of charge generated per unit area on the surface perpendicular to j-direction due to the applied strain in the i-direction. A typical MEMS piezoelectric strain sensor is composed of a piezoelectric material sandwiched between two electrodes with the polar axis, c-axis, perpendicular to the electrodes, as shown in Fig. 3(a). It is assumed that no external electric field is applied. In this configuration, D_3 represents the charges that the electrodes collect due to in-plane stress or strains induced from the substrate. For piezoelectric materials with hexagonal crystal structure, Eq. (12) can be simplified into the following equation

$$D_3 = \frac{Q_3}{A_3} = e_{31}(S_1 + S_2) \tag{13}$$

where Q_3 is the electrode collected charge and A_3 is the electrode area. Notice only normal strains are detected by the piezoelectric sensor in this configuration. All shear strain information is lost because the corresponding e_{ij}'s are zero.

Although it is charge that is generated from the piezoelectric strain sensors, it is simpler and more convenient to measure a sensor output voltage. The voltage output is a function of the capacitance, C, and the resistance, R, of the sensor. This can be modeled by a charge source in parallel with C and R, Fig. 3(b). The voltage output is

$$V = \frac{IR + V_n}{sRC + 1} \tag{14}$$

where V_n is the white thermal noise with spectral density

$$v_n = \sqrt{4 k_B T R} \tag{15}$$

and $I = s\ Q_3 = jw\ Q_3$ is the current through the charge source and V_n is the spectral noise of thermal noise. Constant k_b and variable T are the Boltzmann's constant and sensor temperature in Kelvin. Substitute Eq. (13) into Eq. (14), the voltage can be rewritten as

$$V = \frac{sRA_3 e_{31}}{sRC + 1}(S_1 + S_2) + \frac{1}{sRC + 1} V_n \tag{16}$$

The equation shows that the transfer function from strain input, $S_1 + S_2$, to the measured voltage output is essentially a high pass filter whereas the noise enter the system through a low pass filter. Therefore, it is desirable to use piezoelectric sensors for dynamic signal sensing. At high frequencies, Eq. (16) can be reduced to an algebraic equation as follows

$$V = \frac{e_{31} t}{\epsilon_0 \epsilon_{33}^S}(S_1 + S_2) \quad (17)$$

The capacitance relation, $C = A_3 \frac{\epsilon_0 \epsilon_{33}}{t}$, was used in the above equation where t is the thickness of the sensor piezoelectric layer. The above equation clearly shows that, at higher frequencies, the output voltage is the sum of the in-plane strain times a constant, which is pre-determined by material properties and sensor thickness. Therefore, device sensitivity can be improved by using a thicker piezoelectric layer. At DC or very low frequencies, the sensor contributes to very limited voltage at the output and the response is dominated by thermal noise.

3. SENSOR FABRICATION

3.1. Process Requirements

As we are interested in fabricating strain sensors for use on the steel suspensions in hard disk drives,[11] it is necessary to work with steel substrates at some point during the fabrication process. The suspensions are built from steel sheets ranging from 40 to 200 μm, and the use of such steel substrates is highly unconventional in micro-fabrication, for several reasons. First, the maximum process temperature is limited to 600C or lower. A process temperature higher than the temperature changes the mechanical properties of the substrate. Since the high-temperature deposition and annealing temperature is usually one of the keys in obtaining a high quality semiconductor film, such as polysilicon, the temperature limitation imposes a significant constraint to film qualities.

Secondly, permissible fabrication temperatures may be further limited by the thermal expansion coefficient of steel, which is an order of magnitude larger than most micro-fabrication compatible materials. A non-metal film deposited at an elevated temperature causes tremendous amount of residual strain once the substrate is cooled to room temperature, resulting a warped steel substrate. Not only is it difficult to perform lithography on the warped substrates in the subsequent lithography steps, the deposited film with high residual stress is also prone to delaminate from the steel substrate. Hence, the film is either deposited on the steel substrate at a temperature lower than 300C or fabricated on a separate silicon wafer at high temperature and transferred to the steel substrate afterwards.

Finally, steel substrates can oxidize in the oxygen rich environment, especially at a elevated temperature, and are often very rough compared to typical semiconductor substrates. Therefore, it is important to passivate steel surfaces prior to any high temperature process. Handling of thin steel wafers can also be a challenge, as they are very flexible, which may interfere with deposition uniformity or photolithography accuracy.

3.2. Fabrication of Bonded Amorphous Silicon Piezoresistive Sensors

The bonded polysilicon piezoresistive sensors are fabricated on a standard silicon substrate and transferred to a passivated steel substrate. The sensor fabrication process begins with a 1 μm of phosphosilicate glass layer deposition using low-pressure chemical vapor deposition (LPCVD). This layer serves as the sacrificial layer and also the source of dopants to the polysilicon piezoresistors. Then, 1 μm of undoped polysilicon film, which will be used as the piezoresistive layer, is deposited in LPCVD, following by a low stress LPCVD silicon nitride deposition and patterning, Fig. 4(a)(2). The nitride layer improves the adhesion between the sensors and gold bumps. After patterning, the dopants are diffused from the phosphosilicate layer into the silicon layer in the annealing process at 1000C for one hour, resulting a reasonable uniform dopant concentration,[12] Fig. 4(a)(3). Next, a seed layer is sputtered onto the wafer, Fig. 4(a)(4), after which thick gold bonding bumps are formed by electroplating of the wafer patterned with thick photoresist, Fig. 4(a)(5). The photoresist is then stripped off and the substrate is submerged in 5:1 buffer hydrofluric acid for timed sacrificial layer etching, resulting piezoresistive sensors supported by silicon tethers through anchor points on the silicon substrate, Fig. 4(a)(6).

The steel substrate is passivated by sputtered silicon oxide and amorphous silicon. The oxide is deposited by reactive silicon sputtering in an argon and oxygen environment to provide electrical insulation between

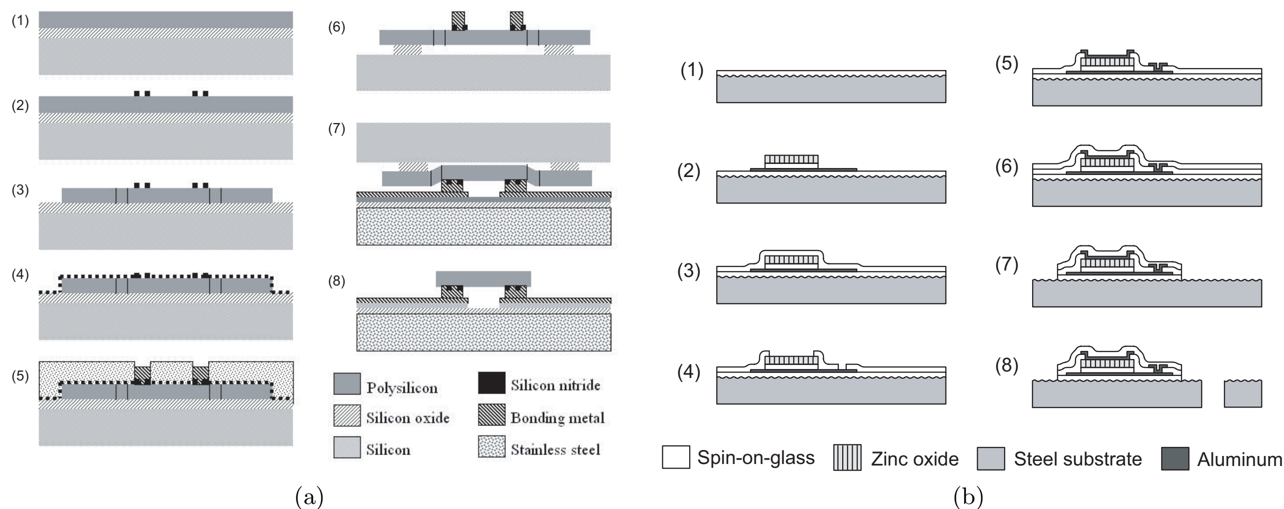

Figure 4. Fabrication processes for (a) polysilicon strain sensors (b) ZnO strain sensors on steel substrate.

substrate and sensor. The silicon layer is formed subsequently by turning off the oxygen flow. This layer provides mechanical strength to withstand forces during the bonding process. Next, a gold layer is evaporated onto the steel substrate that serves as the landing layer for the bonds and as an interconnect layer. After gold patterning, the exposed silicon is removed to eliminate unnecessary material. Finally, the fabricated silicon wafer is bonded face-to-face onto the steel substrate at the gold bumps, Fig. 4(a)(7-8). The bonding process is performed by Microassembly Technologies, Inc. at 80C to minimize sensor buckling after cooling to room temperature.[13] The fabricated polysilicon strain sensors are shown in Fig. 5(a).

3.3. Fabrication of Directly Deposited ZnO Piezoelectric Sensors

A different strategy is adopted to fabricate piezoelectric sensors. Unlike polysilicon, it is possible to directly fabricate piezoelectric sensors on steel substrates because a high quality piezoelectric film can be processed at a lower temperature. The processing temperature depends on the piezoelectric material of choice but is usually less than 600C. For example, ZnO and AlN, two materials commonly used in micro-fabrication are typically sputtered between 300C to 600C. Films deposited at this temperature result a more manageable residual stress. Even in this temperature range, lower temperatures are preferable. As ZnO can be sputtered at a lower temperature than AlN, ZnO is chosen as the material for piezoelectric sensor fabrication. Another common piezoelectric material, lead-zirconate-titanate (PZT), can be manufactured at a slightly higher temperature, with piezoelectric properties orders of magnitudes better than AlN and ZnO. However, it is not an ideal material for micro sensor applications. In addition to a higher processing temperature, PZT's higher relative permittivity causes a lower voltage output in sensor operation, as is evident in Eq. (17), as the ratio e_{31}/ϵ_{33}^S is larger for zinc oxide.

The fabrication process begins with coating a steel wafer with a 0.7 μm spin-on-glass (SOG) insulation layer, Fig. 5(b)(1). The SOG layer prevents the steel substrate from oxidizing in the later high temperature process and reduces surface roughness of the substrate, providing a smooth substrate for ZnO growth. Next, a 0.2 μm aluminum layer is evaporated to form the bottom electrode and connection traces, following by another SOG coating. The second SOG layer serves as the adhesion and buffer layer between the ZnO film to be deposited and the bottom electrode. It is found that the ZnO film does not adhere to aluminum films after cooling from deposition to room temperature well enough to withstand residual stresses caused by thermal expansion coefficient mismatch. The second SOG layer provides better adhesion to both the aluminum layer and ZnO and results in a smoother stress transient between the layers. The ZnO film is deposited at 300C in an argon and oxygen environment. The ZnO and the underlying SOG layer are patterned using wet etching and an SF_6 reactive ion etch (RIE), respectively, Fig. 5(b)(2). After patterning, a third SOG layer is spin-coated to seal the devices, and contact holes are opened from above, Fig. 5(b)(3-4). Next, an aluminum layer is evaporated and

Table 1. Summary of the sensor parameters and experimental results. The sensor length, width and height are in μm. The strain resolution is in nanostrain and gage factor (GF) is unit-less (* = projected).

		Length	Width	Height	Meas. GF	Meas. e_{31}	Resolution
Polysilicon	Standard		20	1	-4.5		130*
	Dogbone	34	20	1	-14.1		70*
ZnO	Normal	700	700	0.8		-0.098	56.9

patterned to form the top electrode, Fig. 5(b)(5). Finally, the sensors are encapsulated using an SOG layer and the substrate is cut into strips for testing, Fig. 5(b)(6-8). A finished ZnO strain is shown in Fig. 5(b).

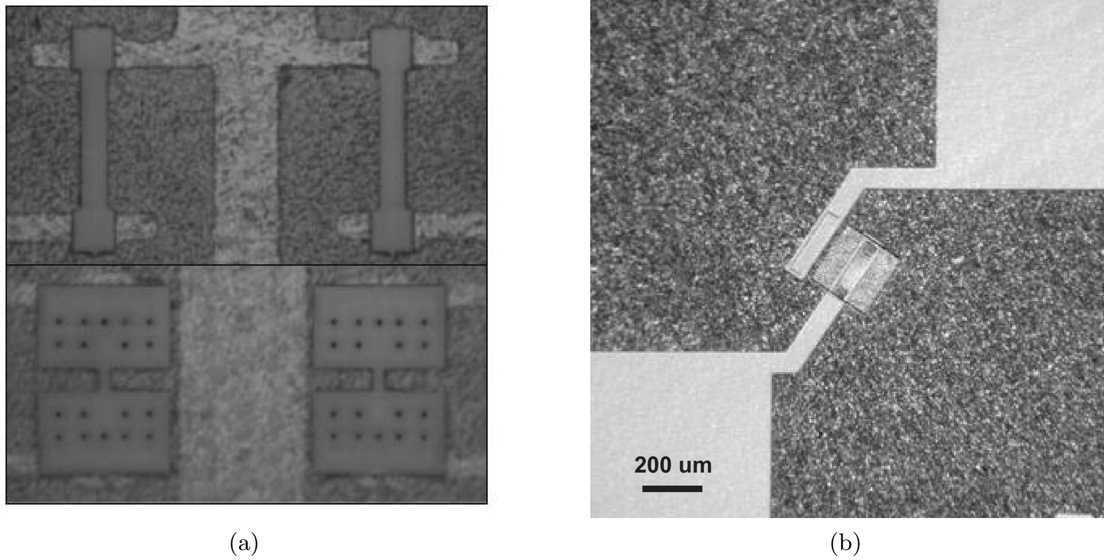

(a) (b)

Figure 5. (a) A fabricated polysilicon strain gage on steel substrate. Top: standard design; bottom: dog-bone design; (b) A fabricated ZnO piezoelectric strain sensor on a steel substrate. Note that the bottom electrode aluminum is skipped on this sensor, and the steel substrate serves as the bottom electrode for signal grounding.

4. EXPERIMENTAL RESULTS AND DISCUSSION

4.1. Sensor Characterization

Slightly different approaches are used to test the fabricated piezoresistive and piezoelectric strain sensors. Both types of sensors are characterized on cantilevers cut from the steel substrates upon which sensors were fabricated or bonded. However, different excitations are applied. For sensitivity testing, a static load may be applied to the steel cantilever tip equipped with bonded piezoresistors whereas an impulse excitation must be applied to cantilevers with piezoelectric sensors. The static load on piezoresistor cantilever allows for simpler testing, but this method dos not work well for ZnO piezoelectric sensors, as they are less sensitivity at low frequencies. Therefore, an impulse is applied to excite the resonance modes of the beam, generating dynamic signal for measurement.

Both approaches are based on beam theory. When a load is applied at the cantilever tip, the tip displacement, v, is measured by a laser Doppler vibrometer (LDV) and the strain, ε, at the sensor location is calculated accordingly. For piezoresistors, the following equations are utilized:

$$P = \frac{3EI}{L_b^3} v \tag{18}$$

$$\varepsilon = \frac{P x_s h_b}{2I} \tag{19}$$

where P, E, I, L_b, h_b and x_s are the applied force, Young's modulus, area moment of inertia of beam cross-section, beam length , beam thickness and sensor location along the beam, respectively. The results of the static deflection tests are shown in Table 1. Without the dog-bone amplification, the measured gage factor is averaged to be approximately -4.5. The value is lower than the anticipated gage factor of a polysilicon beam, which is about -8.9, due to larger than expected nominal resistance. This is believed to be a result of large contact resistances at the bond interface. Using strain amplification from dog-bone sensor geometries, measured gage factor was increased to as high as 14.1, depending on sensor dimensions. While actual testing was done without low noise amplification, these gage factors project to practical strain resolutions ranging from 60 to 150 nanostrain with use of low-noise amplification with input noise 5 nV/$\sqrt{Hz}$ over 20 kHz. (intrinsic resolution limited by thermal noise in the resistors is on the order of 30 nanostrain). To achieve higher resolutions, polysilicon may be replaced by single crystal silicon, with sensors fabricated from silicon-on-insulator wafers.

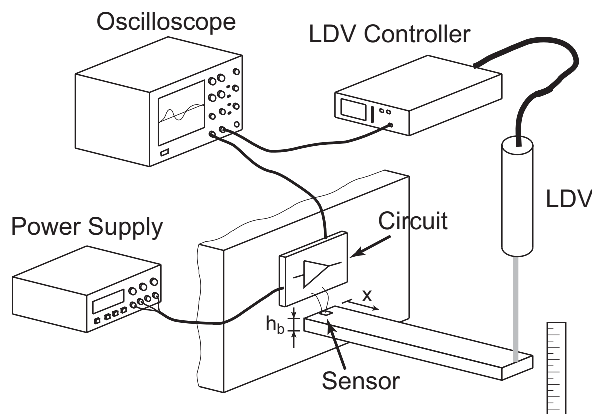

Figure 6. The experimental setup to test both piezoresistive and piezoelectric strain sensors.

A piezoelectric sensor fabricated at the base of a steel cantilever can be tested in a similar way. The applied mechanical impulse excites several modes simultaneously. The shape of each resonance mode is used to calculate the corresponded strain at the base due to the LDV measured tip displacement.[14] The piezoelectric constant, e_{31}, can be evaluated as follows:

$$e_{31} = \frac{2\varepsilon_0 \varepsilon_{33}^S}{y''(x_s = 0) h_b t} \frac{V_o}{G} = \frac{2\varepsilon_0 \varepsilon_{33}^S V_s}{y''(x_s = 0) h_b t} = \frac{\varepsilon_0 \varepsilon_{33}^S V_s}{2 C_n \beta_n^2 \alpha_n h_b t} \tag{20}$$

where C_n is a normalized constant and

$$\alpha_n = \frac{\sin(\beta_n L) + \sinh(\beta_n L)}{\cos(\beta_n L) + \cosh(\beta_n L)} \tag{21}$$

Constants h_b and G are substrate thickness and circuit gain, respectively. V_0, V_s, and y'' are the measured signal after amplification, sensor output before amplification and the second derivative of beam mode shape. The methodology is used to test a fabricated 700 μm squared sensor on an 1.1 cm long and 40 μm thick steel cantilever. The results show that the sensor resolves a peak-to-peak strain signal as good as 57 nanostrain before being buried into noise level. This corresponds to piezoelectric coefficient $e_{31} = -0.098 C/m^2$.

4.2. Discussion

Both piezoelectric and piezoresistive strain sensors have advantages and disadvantages. From a micro-fabrication perspective, while ZnO piezoelectric sensors are easier and cheaper to fabricate on steel substrates, the bonded silicon piezoresistors is more versatile an approach that can also be applied to many types of substrates. In

terms of characteristics, piezoresistive sensors are capable of detecting both dynamic and static load whereas piezoelectric sensors are better at detecting higher frequency signals. As a result, a piezoresistor is a much better choice if the measured strain is inherently very low frequency in nature such as creep. On the other hand, piezoelectric sensor are capable of detecting strains in all directions, depending on the piezoelectric coefficients of a given material. Most piezoelectric sensors are capable of detecting at least three normal strain components simultaneously. Piezoresistors can only detect strain effectively in the direction parallel to the strain sensor, requiring more than one piezoresistor to measure all strain components.

Compared to piezoresistors, piezoelectric sensors are active devices which generate charge due to external strain. The amount of induced charge is proportional to sensor area and piezoelectric coefficients. As the sensor area shrinks, less charge is generated by the sensor for the same external strain input. Very little charge may be generated if the sensors are intended to measure very small vibration signals, on the order of 100 nanostrain. This makes the interface circuit particularly important in order to successfully measure MEMS scale piezoelectric sensors. Typically, the interface circuit has an overall gain of approximately a thousand. With such a large gain, cautions should be taken to minimize any unwant feed-through and noise coming from the environment, as they saturate the circuit very easily. It is very important to place the interface circuit very close to the sensor to reduce environmental noise and parasitic capacitance.

The circuitry for piezoeresistive gage measurement works very different from piezoelectric sensors. A voltage is usually applied across a Wheatstone bridge and an additional stage is used to amplify the signal if needed. As an external voltage source is needed to pass through the sensor, piezoresistive strain gages do not suffer the scaling problem that piezoelectric sensors have. Therefore, these gages can be made approximately ten times smaller and still have decent response. The problem for using MEMS piezoresistive gages to measure very small strain, however, is that the applied current has to pass though the narrow gages, causing the gage temperature to increase. The elevated temperature increases thermal noise which results in noisy measurements. As mentioned earlier, this and lithography limits are the two major factors in determining the sensor size.

5. CONCLUSION

MEMS piezoresistive and piezoelectric strain sensors are prototyped and tested. Novel fabrication processes have been developed to transfer the fabricated silicon piezoresistive sensor onto steel substrates through metal-to-metal bonding and to directly fabricate ZnO piezoelectric sensors on steel substrate. Prototype polysilicon strain gages show consistent sensitivity for both static and dynamics measurements. An innovative dog-bone shape sensor design is implemented to amplify the gage factor through sensor geometry design. For dynamic vibration measurements, the results show ZnO sensors achieve a better sensitivity and resolution over polysilicon piezoresistive strain gages. Both sensors have very promising results with their own advantages and disadvantages. These results can be further improved by using higher quality films with better interface circuits.

6. ACKNOWLEDGMENTS

The work is supported by National Science Foundation (NSF), Information Storage Industry Consortium (INSIC), and Computer Mechanics Laboratory (CML).

REFERENCES

1. A. M. Allen and D. B. Bogy, "Effects of shock on the head-disk interface," *IEEE Transactions on Magnetics* **32**, pp. 3717–3719, September 1996.
2. Y. Huang, M. Banther, P. D. Mathur, and W. C. Messner, "Design and analysis of a high bandwidth disk drive servo system using an instrumented suspension," *IEEE/ASME Transactions on Mechatronics* **4**, pp. 196 – 206, June 1999.
3. J. Juang and G. Rodriguez, "Formulations and applications of large structure actuator and sensor placements," *Proc. YPI&SU/AIAA Symposium on Dynamics and Control of Large Flexible Spacecraft* , pp. 247–262, 1979.
4. K. Hiramoto, H. Doki, and G. Obinata, "Sensor/actuator placement for vibration control using explicit solution of algebraic riccati equation," *J. Sound and Vibrataion* **229**(5), pp. 1057–1075, 2000.

5. C. Y. Kondoh, S. and K.Inoue, "The positioning of sensors and actuators in the vibration of flexible systems," *JSME Int'l J.* **33**, pp. 145–152, 1990.
6. K. Oldham, S. Kon, and R. Horowitz, "Fabrication and optimal strain sensor placement in an instrumented disk drive suspension for vibration suppression," *Proceeding of the 2004 American Control Conference* , pp. 1855–1861, 2004.
7. S. D. Senturia, *Microsystem Design*, Kluwer Academic Publishers, 2000.
8. P. Ciureanu and S. Middelhoek, *Thin film resistive sensors*, Institute of Physics Publishing, 1992.
9. C. Reale, "Size effect on the electrical conductivity and longitudinal gauge factor of thin metal films," *Czechoslovak Journal of Physics* **21**(6), pp. 662–72, 1971. Section B.
10. H. S. Nalwa, ed., *Handbook of Thin Film Materials*, vol. 3, Academic Press, 2002.
11. S. Kon, K. Oldham, R. Ruzicka, and R. Horowitz, "Design and fabrication of a piezoelectric instrumented suspension for hard disk drives," in *Smart Structures and Materials*, V. G. Masayoshi Tomizuka, Chung-Bang Yun, ed., *Sensors and Smart Structures Technologies for Civil, Mechanical, and Aerospace Systems* **6174**, pp. 617430–1–617430–10, March 2006.
12. H. Puchner and S. Selberherr, "An advanced model for dopant diffusion in polysilicon," *IEEE Transactions on Electron Devices* **42**, pp. 1750–4, October 1995.
13. M. M. Maharbiz, M. B. Cohn, R. T. Howe, R. Horowitz, and A. P. Pisano, "Batch micropackaging by compression-bonded wafer-wafer transfer," *Twelfth IEEE International Conference on Micro Electro Mechanical Systems* , pp. 482 – 489, January 1999.
14. S. S. Rao, *Mechanical Vibrations*, Prentice Hall, 1993.